



TITLE:

Far Field condition of Vortex Methods on an
Impulsively Translating Two-Dimensional
Circular Cylinder with
Rotation(Mathematical Analysis of
Phenomena in Fluid and Plasma Dynamics)

AUTHOR(S):

Kida, Teruhiko; Nagata, Toshimi; Nakajima,
Tomoya

CITATION:

Kida, Teruhiko ...[et al]. Far Field condition of Vortex Methods on an Impulsively Translating Two-Dimensional Circular Cylinder with Rotation(Mathematical Analysis of Phenomena in Fluid and Plasma Dynamics). 数理解析研究所講究録 1993, 824: 49-63

ISSUE DATE:

1993-03

URL:

<http://hdl.handle.net/2433/83252>

RIGHT:

Far Field Condition of Vortex Methods on an Impulsively
Translating Two-Dimensional Circular Cylinder with Rotation

木田輝彦 (Teruhiko Kida)
永田俊美 (Toshimi Nagata)
中嶋智也 (Tomoya Nakajima)

Far field condition for steady flows around a two-dimensional rotating circular cylinder is well known, but the condition for transient case is not known well: the circulation around closed curve with very large radius surrounding the cylinder is zero or non-zero, that is, the value of steady case. The condition depends on the initial conditions: (1) the circular cylinder translates impulsively with rotating and (2) the rotating cylinder is started impulsively. The purpose of the present paper is to discuss numerically the influence of the difference of the initial condition to later flows from starting by using the vortex method.

1. Introduction

Unsteady flow around a rotating two dimensional cylinder, traveling through a fluid is of fundamental interest for several reasons; boundary layer control due to Magnus effect [1] and reverse Magnus effect (e.g. [2-4]). Theoretical works concerning this problem are generally based on boundary-layer theory: Badr and Dennis [5] calculated unsteady flow past an impulsively rotating and translating circular cylinder by using the techniques along one used by Collins and Dennis [6], and exhibited the early stages of the formation of a Karman vortex sheet for moderate Reynolds numbers. In their numerical approach,

the circulation round the contour surrounding the cylinder remains zero, as it was at the start. Hence their solutions do not tend to a quasi-steady state rigorously.

The vortex method is an advantage in a sense that the far field condition is imposed easily and essentially, there is no numerical diffusion, and it is essentially reasonable for high Reynolds number flows. From this advantage, there are many works treated high Reynolds number flows past a circular cylinder by the vortex methods (e.g. [7]). However, there are uncertainties of many earlier works in the use of the vortex methods. As one of uncertainties, the prediction of separation has not been calculated rigorously in many works: the Pohlhausen method assuming the attached flow to be quasi-steady [8,9], and the prediction on experimental measurements [4]. Chorin [10] proposed a vortex method by which boundary layer flow can be simulated and he calculated flows past a circular cylinder. Cheer [11,12] extended his approach and obtained the more detailed results. There is not any assumption to predict separation in this vortex method. In works used this vortex method, the conformal mapping technique is used in order to simulate the outer potential flow as exactly as possible.

From these backgrounds, the purpose of the present paper is (1) to discuss the numerical results depending on the far field condition and (2) to study a method by which the vortex method proposed by Chorin [10] is available to various bluff bodies. For the second purpose, we use the panel method proposed by the present authors [13], which has high accuracy near the surface of the body, in stead of the conformal mapping. The availability of

this method will be shown by studying flows around impulsive starting circular cylinder without rotation. For the first purpose, an impulsive translating circular cylinder with rotation is treated in this paper. The far field condition of zero circulation treated in [4,5] sounds to be reasonable for impulsive rotating and impulsive translating problem, as initial flow is rest. In the case that a rotating circular cylinder with constant angular velocity starts impulsively, initial circulatory potential flow is the exact solution of the Navier-Stokes equation, so that the far field condition must be non zero circulation condition at the time of termination of the calculation. The limiting case of this problem for time being infinite seems to be the same as that of early works [4,5] physically, although solutions of the Navier-Stokes equation for the above two problems are considered to be different from the point of view of the mathematical analysis (e.g. [14]). The present paper will discuss this difference by using the vortex method.

2. Far Field Condition

We consider two initial cases: (1) A circular cylinder starts and rotates impulsively and (2) a rotating circular cylinder starts impulsively. We take the orthogonal coordinate system fixed with the center of the circular cylinder by (x_1, x_2) , and t by time. The surface of the circular cylinder is denoted by $(x_1^2 + x_2^2)^{1/2} = 1$. The initial conditions for two cases are respectively given by

Case (1): $\vec{u} = 0 \quad (t < 0)$

$$\vec{u}=(\Omega \sin \theta,-\Omega \cos \theta) \quad (r=1 \text { and } t \geq 0)$$

$$\vec{u}=(1,0) \quad (t \geq 0) \text { as } r \rightarrow \infty$$

$$\text{Case (2): } \vec{u}=(\Omega \sin \theta,-\Omega \cos \theta) \quad (r=1 \text { and any } t) \quad (1)$$

$$\vec{u}=(0,0) \quad (t < 0) \text { as } r \rightarrow \infty$$

$$\vec{u}=(1,0) \quad (t \geq 0) \text { as } r \rightarrow \infty$$

where $(x_1, x_2)=(r \cos \theta, r \sin \theta)$ and Ω is clockwise angular velocity.

From far field condition, we have

$$\text{Case (1): } \int_{S_{\infty}} \vec{u} \cdot d\vec{s} = 0$$

$$\text{Case (2): } \int_{S_{\infty}} \vec{u} \cdot d\vec{s} = -2\pi\Omega \equiv \Gamma_0 \quad (2)$$

where S_{∞} is the circle with radius being infinite and s is the arc length along the circle. Suppose that vorticity decays with r , then far field conditions given by Eq.(2) hold for any time. Let Γ_s and Γ_p denote the circulation due to the shedding vortices and around the surface of the body respectively. Since $\Gamma_s + \Gamma_p = 0$ for Case (1) and $\Gamma_s + \Gamma_p = \Gamma_0$ for Case (2) initially, these relations are hold for any time:

$$\text{Case (1): } \Gamma_s + \Gamma_p = 0 \quad (3)$$

$$\text{Case (2): } \Gamma_s + \Gamma_p = \Gamma_0$$

3. Vortex Method and Numerical Approach

The vortex method used in the present paper is essentially the same as that used by Cheer [11,12]. The present authors [15] study this method proposed by Chorin [10] and clear the concept of the vortex-sheet element: Near the surface of the cylinder, the main flow is directed almost to tangential direction on the surface of the cylinder, so that we have to divide the integral

area for the discretization of vorticity field such that the width of the longitudinal direction is much wider than the lateral one.

The numerical approach of this method is the fractional method: We first solve the outer inviscid flow by using the panel method, second we create vortex-sheet elements from no-slip boundary condition, and finally we advect all vortices as material particles. In this time, random walk method is used for the viscous diffusion: Its variance is $2\Delta t/R_e$ (in the present calculation Δt is taken as 0.1), where R_e is the Reynolds number based on the diameter of the circular cylinder and the constant translating velocity. In the present paper, panels are consisted of equi-polar angle and the number of panels is taken as M being equal to 40.

The vortex-sheet elements have to be distributed in the boundary layer, so in the present calculation the maximum width of the boundary layer, H , is taken as $2/R_e^{1/2}$. The length of the vortex-sheet element is taken as l equal to $2\pi/M$. The induced tangential velocity u due to the vortex-sheet element is given by [11 or 15];

$$u = \begin{cases} 0 & : \text{upper side of vortex-sheet} \\ \xi d/l & : \text{lower side of vortex-sheet} \end{cases} \quad (4)$$

where ξ is the circulation per unit length of this vortex-sheet element and d is the length of the part of the vortex-sheet element which is in the collocation panel, as shown in Fig.1. The normal induced velocity is obtained from the integration

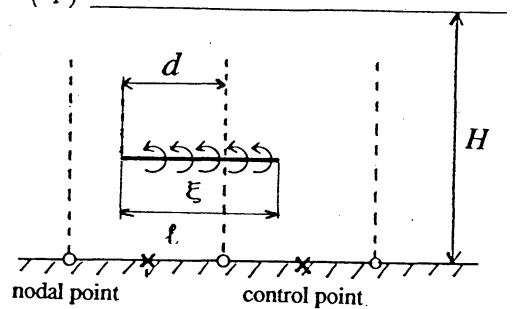


Fig.1. Vortex-sheet element

of the continuity equation by applying the finite difference of first order for tangential velocity.

The creation of the vortex-sheet elements is done by the no-slip condition: We first obtain the slip velocity on the surface of the cylinder and second we create them from no-slip condition. The tangential velocity at the edge of the maximum width of the boundary layer is obtained from the panel method, the tangential velocity due to the vortex-sheet elements in the boundary layer is added, and finally we can obtain the slip velocity on the surface of the cylinder. We note that provided the outer flow is obtained from the flow tangency condition on the surface of the circular cylinder, the normal condition on the surface of the cylinder is satisfied essentially. We define the slip velocity on the surface by u_s . Then we use the following vorticity creation algorithm: We set the maximum circulation per unit length of the vortex-sheet element as $\xi_{\max}=0.2$, according to Cheer [11]. If $2u_s$ is less than ξ_{\max} , we create the vortex-sheet element on the surface of the cylinder whose strength is $2u_s$. If $2u_s$ is larger than ξ_{\max} , we create the vortex-sheet element on the surface of the cylinder whose strength and number are ξ_{\max} and $[2u_s/\xi_{\max}]$ respectively, where $[]$ is Gauss symbol. The reason why the 2 times of the slip velocity is used is caused from the use of the random walk method for the viscous diffusion.

Vortex-sheet elements in the boundary layer and vortex blobs in the outer flow are advected as material particles. Then, there are cases that a vortex-sheet element flows out from the boundary layer or a vortex blob flows into the boundary layer. In these cases, the vortex-sheet element changes to the vortex blob and

vice versa. We use the relation between l and σ : $\sigma=l/\pi$, where σ is the cut-off radius of the vortex blob. When the cut-off area of the vortex blob contacts on the surface of the cylinder just, the tangential velocity at the contact point induced by the vortex blob is $\sigma\omega$, where ω is vorticity of the vortex blob, on the other hand, the tangential one induced by the vortex-sheet element is ξ , so that these velocities must be same: $\sigma\omega=\xi$. Further, we have to conserve the circulation: $\pi\sigma^2\omega=\xi l$. Thus, we have obtained the above relation.

Let us consider aerodynamic forces. Forces acted on the cylinder due to the pressure is obtained from the modified Bernoulli's equation, because the pressure on the surface of the cylinder is identical with that on the outer edge of the boundary layer. Therefore, we have

$$X+iY=i\int_{S_b} p dz$$

where X and Y are the x_1 and x_2 components of the pressure force of the cylinder, S_b is the outer edge of the boundary layer around the cylinder, and $z=x_1+ix_2$. Outer flows are treated as potential flow except vortex blobs. We finally have

$$X+iY=-i\rho\int_{S_b} \frac{\partial\phi}{\partial t} dz - \frac{i}{2}\rho\int_{S_b} \left(\frac{dF}{dz}\right)^2 d\bar{z}$$

where F is the complex potential, ϕ is the velocity potential, and "-" denotes the conjugate. From this formula, we have a little different expression of pressure force with regard to the far field condition:

Case (1) :

$$X=2\pi\rho\text{Real}(\dot{a}_1)+\rho\frac{\Gamma_c y_c}{\Delta t} +\rho\sum_j \Gamma_j v_j \quad Y=2\pi\rho\text{Imag}(\dot{a}_1)-\rho\frac{\Gamma_c x_c}{\Delta t} -\rho\sum_j \Gamma_j u_j$$

Case (2) :

(5)

$$\chi = 2\pi\rho \text{Real}(\dot{a}_1) + \rho \frac{\Gamma_c y_c}{\Delta t} + \rho \sum_j \Gamma_j v_j \quad \gamma = 2\pi\rho \text{Imag}(\dot{a}_1) - \rho \frac{\Gamma_c x_c}{\Delta t} - \rho \sum_j \Gamma_j u_j - \rho \Gamma_o$$

where Γ_j is the circulation of the vortex blob, (u_j, v_j) is the velocity of Γ_j , ρ is the density of fluid, Γ_c and (x_c, y_c) are the circulation of the shedding vortex blob from the boundary layer in the lapse of small time Δt and its position respectively. \dot{a}_1 is the derivative of a_1 with respect to t , where a_1 is given by

$$a_1 \equiv - \frac{1}{2\pi} \int_{S_b} \kappa(s) z(s) ds - \frac{i}{2\pi} \int_{S_b} \gamma(s) z(s) ds$$

where κ and γ are the source and constant circulation distribution per unit length on the surface of the cylinder respectively, in order to solve the outer flow by panel method. We note that Γ_p in Eq.(3) is given by: $\Gamma_p = -2\pi\gamma$. The friction force may be obtained by Chorin's method [10], but its value is very small, compared with the pressure drag, so in the present paper we discuss on the pressure force only.

4. Numerical Results

The numerical results of vortex blobs and the streamlines are shown in Fig.2 in the case of impulsively translating without rotation and time $t=40$. We note that the separation points are automatically determined. Comparing with results given by Anderson et al. [16], we see that the present method is available and almost comparable with the method using conformal mapping.

The numerical results of vortex blobs and streamlines for Cases (1) and (2) are shown in Fig.3. We see that the figure of vortex blobs is different: For both cases, the similar pattern

such like Karman vortex sheet is obtained but the number of clusters is different. The position of vortex blobs for Case (2)

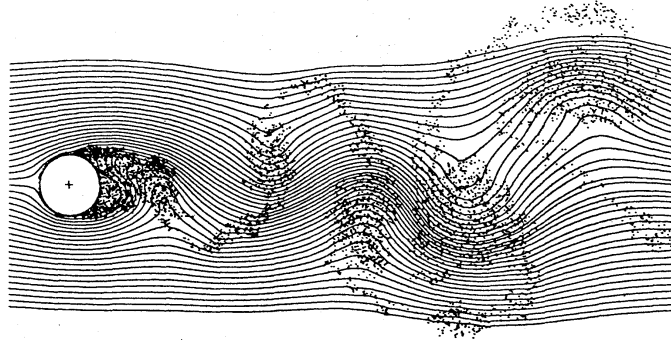
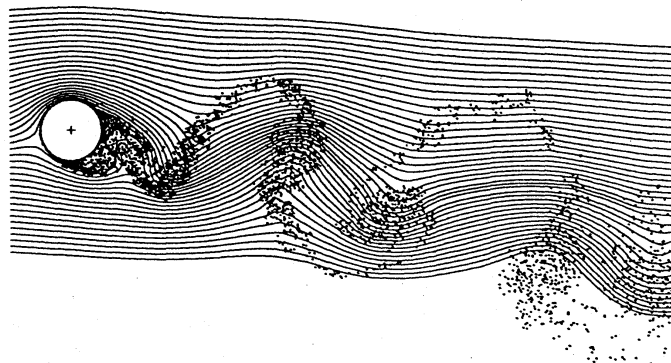


Fig.2. Vortex blobs and streamlines without rotation ($t=40$)

Case (1)



Case (2)

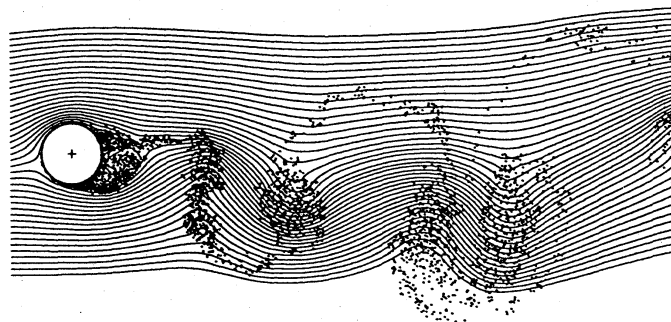


Fig.3. Vortex blobs and streamlines with rotation ($t=25$)

is a little upward and the downwash velocity of clusters for Case (1) is a little larger than that for Case (2). Figure 4 shows vortex blobs and streamlines at an early time ($t=5$). We see that there is a cluster of vortices in Case(2) but in Case(1) an

initial cluster is just forming: This is the difference of number of clusters, and the difference of downwash velocity seems to be caused by the difference of early stages.

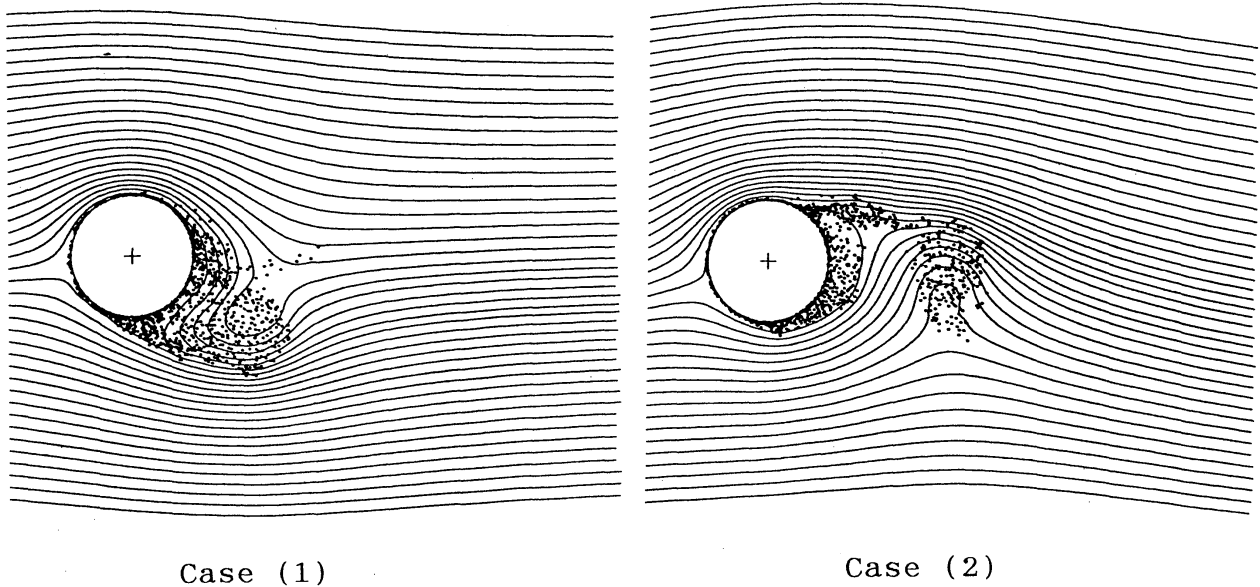


Fig.4. Early stages with rotation ($t=5$)

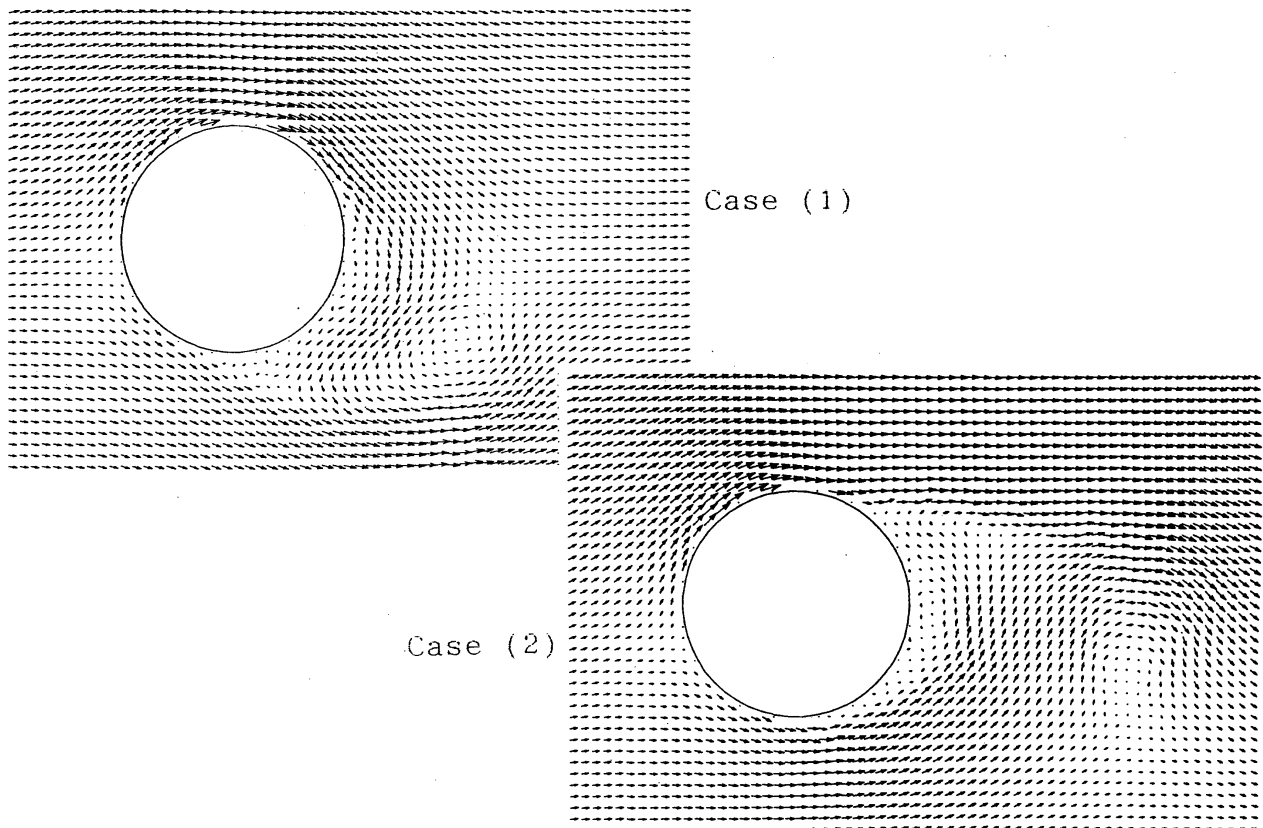


Fig.5. Velocity vectors of early stages ($t=5$)

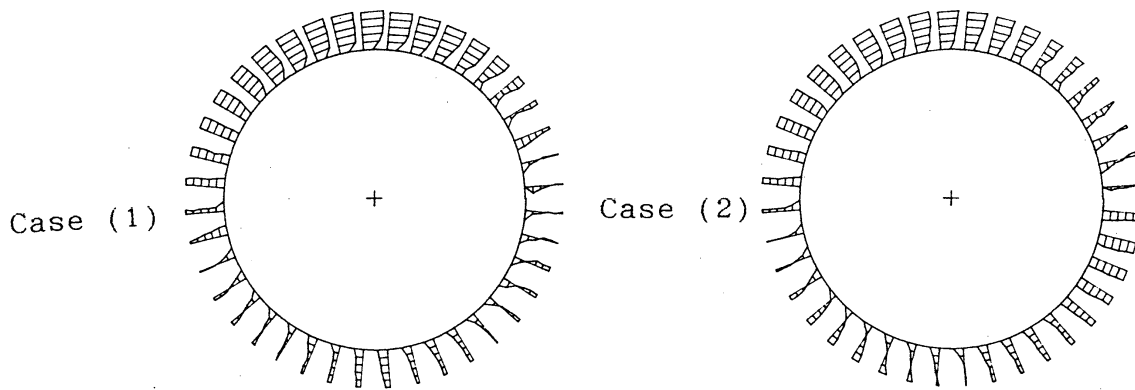


Fig.6. Velocity profile in the boundary layer ($t=25$)

The detailed velocity vector of early stages is also shown in Fig.5. The velocity profiles in the boundary layer are shown in Fig.6. We see from these figures 5 and 6 that flows of both cases are different at the same time. Figure 7 shows the feature of flow in the case where the lift coefficient is almost valley (see in Fig.8), and we see that they are almost similar.

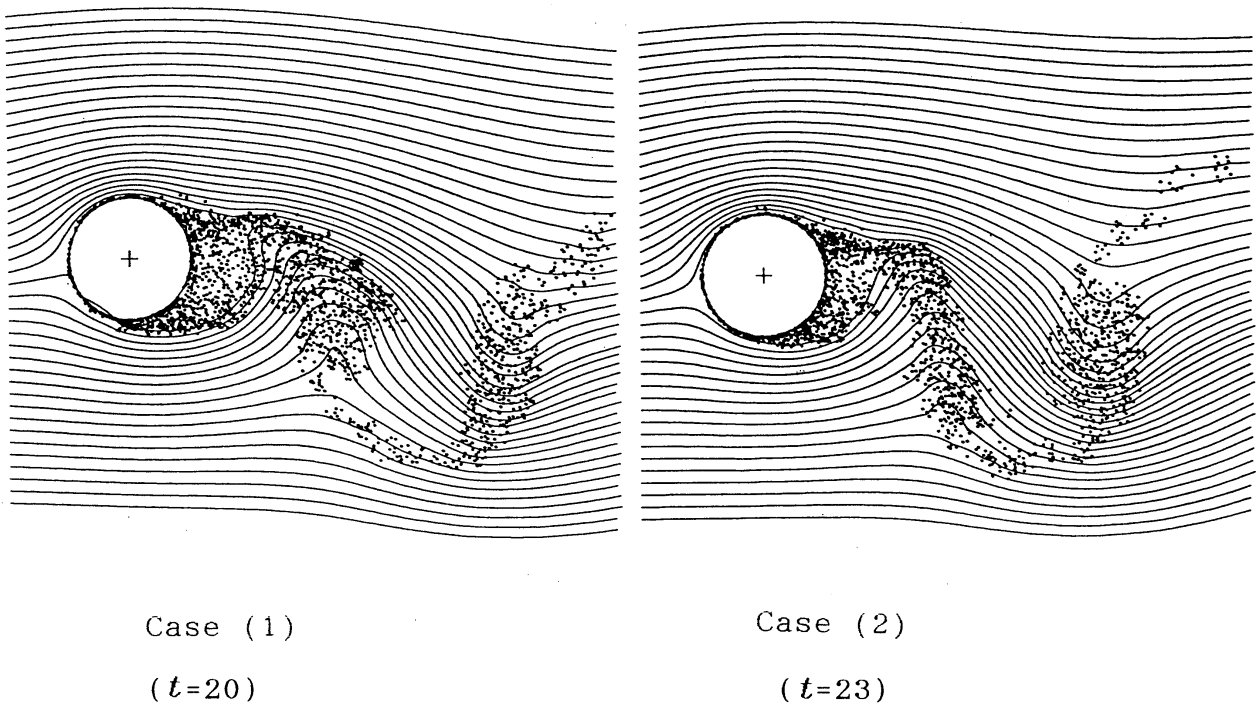


Fig.7. Vortex blobs and streamlines for almost valley lift

The lift and drag forces due to the pressure are shown in Fig.8. C_l and C_d are the lift and drag coefficient, respectively, based on the translating velocity and diameter of circular cylinder. From this figure, we see that the drag force is almost same and the lift force is almost same except initial few steps, although, as pointed out in section 3, the formula of lift force, Eq.(5), is different. To know the dominant term of this result, we divide lift force given by Eq.(5) into two terms; shedding vortex and a_1 term, $C_l(\text{vortex})$ and $C_l(\text{source})$. Figure 9 is the results of these two terms. From this figure, we see that the shedding term for Case (2) is smaller than that for Case (1) and this discrepancy is supplemented by the fourth term of Eq.(5) due to the far field condition.

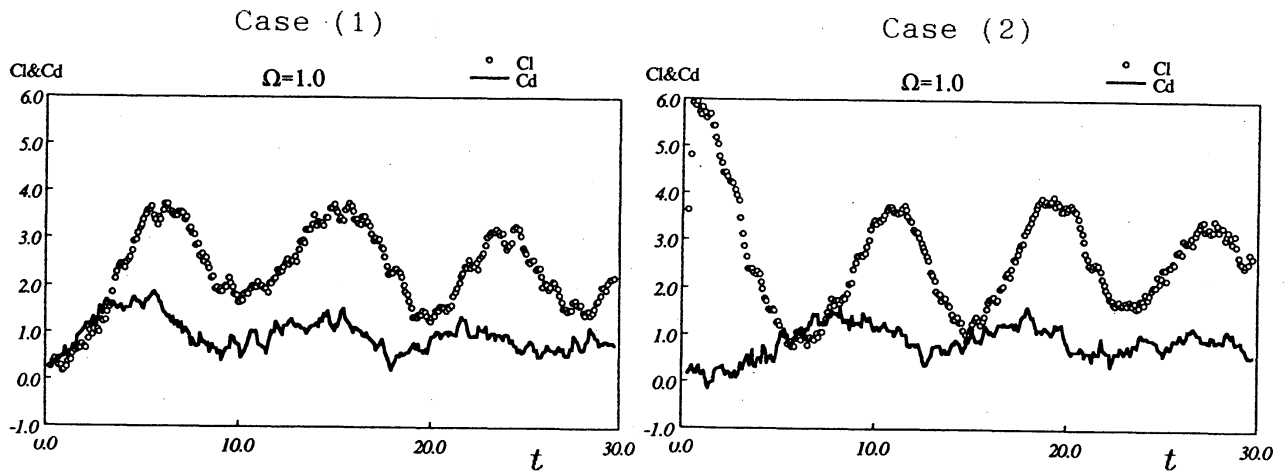


Fig.8. Lift and drag coefficients

Figure 10 is the time histories of the circulation, Γ_p , for both cases. We see that Γ_p is almost same except initial few steps. From this fact, we may arrive at: The total circulation in the boundary layer is almost same, because the circulation around the outer edge of the boundary layer is Γ_p and the circulation around

the surface of the circular cylinder is Γ_0 .

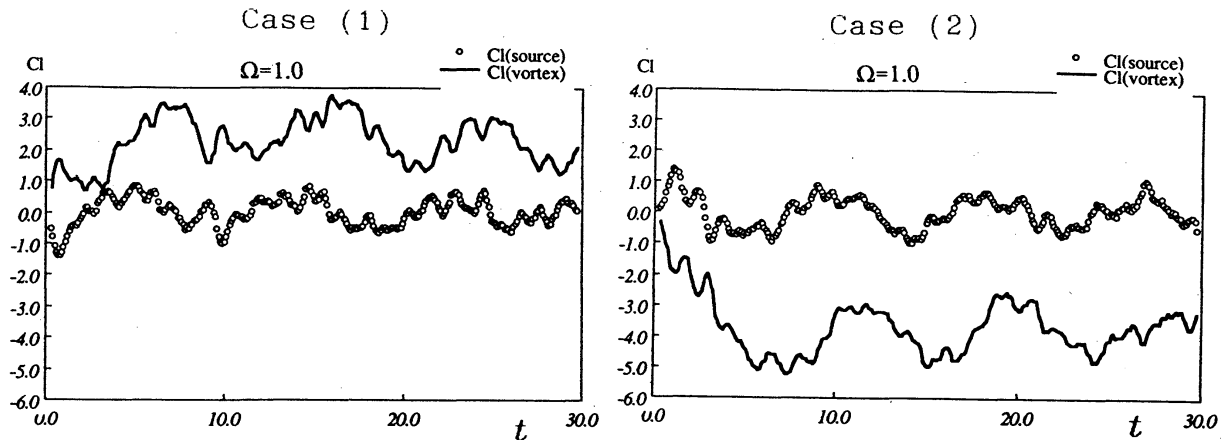


Fig.9. Lift components of shedding vortex and others

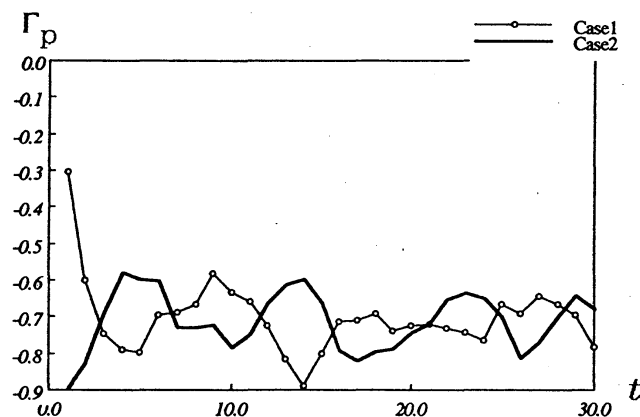


Fig.10. Time history of circulation Γ_p

This fact implies the possibility that the initial cluster of vortices in Case (2) acts the cancel of the last term of Eq.(5), which is derived by the far field condition. The total circulation of initial cluster for Case (2) shown in Fig.4 is almost -5.24. If this cluster flows down with translating velocity, the above mentioned fact may be confirmed. From these results, we may arrive at the following conclusion, although we can't say surely: The difference of initial condition is not so important except initial few time steps and this difference

appears such like the starting vortex, provided the limiting boundary condition as $t \rightarrow \infty$ is the same.

6. Conclusions

The present paper proposes an alternative numerical method on vortex methods; the combination of the vortex method with the panel method. The numerical results shows that this method is comparable with earlier results, so that it may be applied to bluff bodies with complicated shapes.

Two different initial conditions of impulsively translating circular cylinder with rotation are calculated numerically: There is difference of flows at the same time step, but the pressure force is almost same except initial few time steps. The reason of this latter fact is discussed and is shown that the initial cluster of vortices plays a role just like a starting vortex around an impulsively starting aerofoil. This fact implies that the initial condition is not so important except early time stages, if the boundary condition as $t \rightarrow \infty$ is the same.

Acknowledgment: The present authors express sincere thanks to Prof. Tsutahara (Kobe University) for pointing out that the difference of the far field condition seems to be only starting vortex.

References

- [1] Swanson, W.M., Trans. ASME, Basic Engrs., 83, 1961, pp.461-470
- [2] Ericsson, L.E., AIAA J., 18, 1980, pp.935-944
- [3] Matui, T., J. Japan Soc. Aero. Space Sci., 20, 1972, pp.18-26
- [4] Kimura, T. and Tsutahara, M., AIAA J., 25, 1987, pp.182-184

- [5] Badr, H.M. and Dennis, S.C.R., J. Fluid Mech., 158, 1985, pp.447-488
- [6] Collins, W.M. and Dennis, S.C.R., J. Fluid Mech., 60, 1973, pp.105-127
- [7] Sarpkaya, T., Trans. ASME, J. Fluid Engrs., 11, 1989, pp.5-52
- [8] Sarpkaya, T. and Shoaff, R.L., AIAA J., 17, 1979, pp.1193-1200
- [9] Inamuro, T. and Adati, T., Trans. JSME, B 52-476, 1986, pp.1600-1607
- [10] Chorin, A.J., J. Fluid Mech., 57, 1973, pp.785-796
- [11] Cheer, A.Y., SIAM J. Sci. Stat. Comp., 4, 1983, pp.685-705
- [12] Cheer, A.Y., J. Fluid Mech., 201, 1989, pp.485-505
- [13] Kida, T., Nagata, T. and Nakajima, T., will be published on Comp. Fluid Dynamics J.
- [14] Fujita, H. and Kato, T., Arch. Rat. Mech. Anal., 16, 1964, pp.269-315
- [15] Kida, T. and Nakajima, T., Turbomachinery, 12, 1992, pp.781-788
- [16] Anderson, C.R., et al., Phys. Fluids, A-2, 1990, pp.883-885